Non L-type voltage dependent calcium channels control vascular tone of the rat basilar artery

Manuel F. Navarro-Gonzalez[‡], T. Hilton Grayson[‡], Kate R. Meaney[‡], Leanne L. Cribbs[§] and Caryl E. Hill[‡]

[‡]Division of Neuroscience John Curtin School of Medical Research, Australian National University, Canberra, ACT, Australia and [§]Cardiovascular Institute, Loyola University Medical Center, Maywood, IL 60153 USA

Summary

1. Constriction of cerebral arteries is considered to depend on L-type voltage-dependent calcium channels (VDCCs), however many previous studies have used antagonists with potential non-selective actions. Our aim was to determine the expression and function of VDCCs in the rat basilar artery.

2. The relative expression of VDCC subtypes was assessed using quantitative PCR and immunohistochemistry and the data were correlated with physiological studies of vascular function. Domains I to II of the T channel subtypes expressed in the rat basilar artery were cloned and sequenced.

3. Blockade of L-type channels with nifedipine had no effect on vascular tone. In contrast, in the presence of nifedipine, hyperpolarization of short arterial segments produced relaxation, while depolarization of quiescent segments evoked constriction.

4. mRNA and protein for L- and T-type VDCCs were strongly expressed in the main basilar artery and side branches, with $Ca_V3.1$ and $Ca_V1.2$ the predominant subtypes.

5. T-type VDCC blockers, mibefradil, pimozide and flunarizine, decreased intracellular calcium in smooth muscle cells, relaxed and hyperpolarized arteries, while nickel chloride (100 μM) had no effect. In contrast to nifedipine, nimodipine produced hyperpolarization and relaxation.

6. When arteries were relaxed with U73122 (phospholipase-C inhibitor), in the presence of nifedipine, 40 mM KCl evoked depolarization and constriction, which was significantly reduced by mibefradil.

7. Sequencing of domains I-II revealed splice variants of $Ca_V3.1$ which may impact on channel activity.

8. We conclude that vascular tone of the rat basilar artery results from calcium influx through nifedipine-insensitive VDCCs with pharmacology consistent with $Ca_V3.1$, T-type channels.

Introduction

Voltage dependent calcium channels (VDCCs) are transmembrane proteins which provide influx of calcium for a variety of intracellular activities in excitable cells. In blood vessels, this calcium entry produces vasoconstriction and blockers of VDCCs have been used to treat cardiovascular disorders. VDCCs consist of different subunits, the α1 subunit, which contains 4 homologous transmembrane domains encompassing the pore, the voltage sensor and the selectivity filter, and the auxiliary subunits β, α2δ and γ. The α1 subunits have been classified as $Ca_V1.1$, $Ca_V1.2$, $Ca_V1.3$, $Ca_V1.4$ (L-type VDCCs), $Ca_V2.1$ (P/Q-type VDCCs), $Ca_V2.2$ (N-type VDCCs), $Ca_V2.3$ (R-type VDCCs), $Ca_V3.1$, $Ca_V3.2$ and $Ca_V3.3$ (T-type VDCCs) (see Table 1 for details; for reviews see Perez-Reyes, 2003[1]; Lacinová, 2005[2]). The T-type or transient, rapidly inactivating VDCCs possess a lower membrane potential threshold for activation than the other channel subtypes (~−70 mV), and hence are called low voltage activated; the remaining seven channels being high voltage activated.[2] Interestingly, the T-type currents recorded from many vascular smooth muscles are activated at more positive voltages (−30 to −50 mV) and are inactivated more slowly than those in other tissues.[1]

Traditionally, it is believed that L-type or long lasting VDCCs control tone of cerebral arteries, such as the basilar artery, as these channels would be open and stay open at the membrane potentials experienced by vascular smooth muscle *in vivo* (−30 to −50 mV). The most reliable studies have involved the specific L-type VDCC blocker, nifedipine, which decreased agonist-induced vascular tone in the basilar artery of the dog,[3-5] rat,[6,7] and rabbit,[8,9] as well as spontaneously acquired tone in the dog[10] and rabbit.[11] Nevertheless, nifedipine did not completely reverse agonist-induced contraction of basilar arteries of adult rats,[6] dogs[4] and rabbits,[9] nor did it decrease vascular tone of the basilar artery in young rats.[12]

Many other studies, in which L-type VDCCs have been suggested to control vascular tone of the basilar artery, have used VDCC blockers such as nimodipine.[13-21] Indeed, nimodipine has been the most commonly used dihydropyridine in studies conducted *in vivo* which have demonstrated control of pial vessel diameter.[22] However, nimodipine has been shown to block nifedipine-insensitive VDCCs, in addition to typical L-type channels[23-26] and is more potent than nifedipine in decreasing agonist-induced vasoconstriction in cerebral arteries.[16,18,27] Together, these data suggest that other VDCCs could be involved in the regulation of cerebrovascular tone and could explain why L-type blockers do not decrease vasoconstriction during vasospasm,[5,28] although nimodipine is effective.[29]

Recently, L, T and N-type VDCCs were identified and electrophysiologically characterized in whole cell patch clamp studies using isolated smooth muscle cells of the dog

Table 1. Subtypes and functional expression of VDCCs.

Family	Former name	Structural nomenclature	Antagonists	Common location
L	α_{1S}	$Ca_V1.1$	Dihydropyridines e.g. Nifedipine Nisoldipine Nimodipine Phenylalkylamines e.g. Verapamil Benzothiazepines e.g. Diltiazem	Cardiovascular system
	α_{1C}	$Ca_V1.2$		
	α_{1D}	$Ca_V1.3$		
	α_{1F}	$Ca_V1.4$		
P/Q	α_{1A}	$Ca_V2.1$	ω-agatoxin IVA ω-agatoxin IVB ω-conotoxin MVIIC	Brain
N	α_{1B}	$Ca_V2.2$	ω-conotoxin GVIA ω-conotoxin MVIIA	
R	α_{1E}	$Ca_V2.3$	SNX-482	
T	α_{1G}	$Ca_V3.1$	Mibefradil Pimozide Nickel chloride Kurtoxin Flunarizine Nimodipine	Brain Cardiovascular system
	α_{1H}	$Ca_V3.2$		
	α_{1I}	$Ca_V3.3$		

basilar artery.[17] However, isometric tension studies to identify the physiological significance of these currents were inconclusive as they were conducted in the presence of concentrations of nimodipine and mibefradil[17] that would have mixed actions on both L and T-type channels.[23] The aim of the present study was therefore to investigate the functional significance of VDCC subtypes in the intact rat basilar artery and its smaller side branches, using nifedipine to specifically block L-type VDCCs. We have also determined the relative expression of VDCC subtypes using quantitative PCR and immunohistochemistry and correlated these data with physiological studies of vascular function. Finally, we have cloned and sequenced domains I to II of the T channel subtypes expressed in the rat basilar artery, as previous mutagenesis studies have identified these regions as containing sequences which may alter voltage gating, speed of inactivation and surface expression of the channels.[30,31]

Methods

All experiments were performed in accordance with a protocol approved by the Animal Experimentation Ethics Committee of the Australian National University. Male Wistar rats aged 14-17 days were anaesthetized with ether and euthanized by decapitation. The brain was gently removed and placed in cold isolated vessel dissecting buffer (IVDB) containing (mM): 3 3-(N-morpholino) propanesulphonic acid (MOPS); 1.2 NaH_2PO_4; 4.6 glucose; 2 pyruvate; 0.02 EDTA(Na); 0.15 albumin; 145 NaCl; 4.7 KCl; 2 $CaCl_2$; 1.2 $MgSO_4$. A rectangular section of the meninges, containing the basilar artery and its main and secondary branches was isolated.

Electrophysiological studies

The pia was pinned firmly over the vessels to facilitate stable intracellular impalements. Segments of the primary branch of the basilar artery were cut to lengths of 300-500 μm to enable changes in membrane voltage by current injection. Intracellular voltage recordings were made in continuous current clamp mode (Axoclamp 2B, Axon Instruments, USA), using sharp intracellular microelectrodes (100-200 MΩ, 0.5 M KCl). Resting membrane potential (RMP) was defined as the most negative membrane potential during membrane voltage oscillations. Current application was performed using the single electrode discontinuous current clamp mode and slow switching frequencies of 300Hz. Electrode capacitance was minimized by keeping solution levels low, dipping the electrode tips in silicone and compensated by monitoring the head stage voltage. Hyperpolarizing and depolarizing current steps were applied. Recordings were low-pass filtered (cut off frequency of 100 Hz). Recordings of membrane potential and diameter changes were acquired simultaneously in the region where the cell was impaled at sample rates of 200 Hz. Experiments were performed in Krebs solution at 33-34°C as previously described.[12]

Calcium imaging

The pia was gently removed from the arteries, which were pinned in a narrow well created in a sylgard (Dow Corning Corporation, USA) coated coverslip, in a 1 mL recording chamber. Preparations were incubated in 5 μM Fura-2 acetoxymethyl ester (Fura-2 AM) and measurements of changes in intracellular calcium concentration made as

Table 2. Ca_V Primer sequences.

Channel	PCR Primers 5′-3′ Forward (above), Reverse (below)	Expected Product Size
$Ca_V1.1$	CCAATAAGATCCGCGTCCTATGTC	146 bp
	CAAGGATCTGATTCCTCATGGAGT	
$Ca_V1.2$	GAAGATTGCCCTGAATGACACCAC	160 bp
	CAGACTCTGGAGCACACTTCTTGC	
$Ca_V1.3$	TCCAGCAGGAAATTCGGTGTGTCA	189 bp
	TCGGTCGTGCTTGTAGGAGTAATG	
$Ca_V1.4$	AACTGGGCCTAGTGATGATGATGG	186 bp
	AGGGACTTCCTGTTCCTCATTCTG	
$Ca_V2.1$	TCAAGAAAGCAGCATGAAGGAGAG	181 bp
	CGCTGTCTGAGTAGCCATCAGTTC	
$Ca_V2.2$	TGATGGCACCAGCATCAACCGACA	122 bp
	TTGCCCAGGCAAGACAGCATGATT	
$Ca_V2.3$	TCGGAGTGGATACCCTTCAATGAG	107 bp
	AGCGATTGCTGTTCCTGGAATTGT	
$Ca_V3.1$	AGTCAGGCTCCATCTTGTCCGTTC	204 bp
	TCCAGGGAGTCAGTCCTTATTGCT	
$Ca_V3.2$	CGACCAAGTTCCATGACTGCAACG	145 bp
	CAGCACTTTGTGTAGACGGAAGCA	
$Ca_V3.3$	GCACGAGGACTGCAATGGCAGAAT	120 bp
	CCGGAAACACAGGGTATAGTCGAT	
3.1 domain I	TAGCTTCACGCAGCTCAACGACCT	1215 bp
	GTGCTAGCATTGGACAGGAATCGT	
3.1 I-II Linker	CAACACCACCTGTGTCAACTGGAA	1269 bp
	AGCCTCCAGAAAGCCAGCACAGAA	
3.1 domain II	GGCTTTCTGGAGGCTGATCTGTGA	856 bp
	GCTCTTTCGTAGTTCCGCGTGTTC	925 bp
3.2 domain I	AGCTCTGGCTGCCACAGTCTTCTT	1267 bp
	GGTACTGCTGGGATCCACCTTCTT	
3.2 I-II Linker	ACAACATTGGCTACGCTTGGATTG	1069 bp
	TCTGAGCCACTGAATTCAAACTCG	
3.2 domain II	GTGAGCTGAAGAGCTGCCCATATT	1014 bp
	TAGACGTCTTATCCTCGTCGGTGT	

previously described.[12] Change in calcium concentration was determined by the ratio of the fluorescence emission recorded at 510 nm following alternate 340 and 380 nm excitation ($F_{340/380}$). In some experiments calcium was measured in the same preparation as intracellular voltage recordings by making a small hole in the overlying pia for access of the Fura-2 AM.

Measurement of vessel diameter

Diameter was simultaneously measured with DIAMTRAK, an edge-tracking computer program.[32] When combined with calcium imaging studies, images were collected under infrared illumination (Hamamatsu High Performance Vidicon Camera, Japan).

Drugs and solutions

As there are no highly selective T-type blockers currently available, we have used 3 structurally different drugs, mibefradil, pimozide and flunarizine, which have been shown to block T-type channels.[23] Mibefradil blocks T-type currents in vascular smooth muscle (IC_{50} 0.1-0.2 μM), but can inhibit L-type channels at concentrations > 1μM.[23] Mibefradil was therefore used at 1 μM as previously shown.[33,34] Concentrations of the other drugs were chosen on the basis of T-type channel blockade in other studies: pimozide 10 μM,[35,36] flunarizine 100 μM.[2,36] Nifedipine was used to block L-type VDCCs (1, 10 μM). $NiCl_2$ (100 μM) was used to differentiate the actions of $Ca_V3.2$ channels (IC_{50} 13 μM), from $Ca_V3.1$ and $Ca_V3.3$ (IC_{50} 250 μM[37]).

Sources of drugs were: 1-(6-((17β-3-methoxyestra-1, 3,5(10)-trien-17-yl) amino) hexyl)-1H-pyrrole-2,5-dione (U73122; Phospholipase C inhibitor) (BIOMOL, PA USA); nifedipine, nimodipine, mibefradil (Sigma Chemical Co., MO USA); 2-aminoethyldiphenyl borate (2-APB; IP_3 receptor inhibitor) (Calbiochem, Germany); nickel chloride (BDH Laboratory Supplies, England), pimozide (Sigma Chemical Co., MO USA), flunarizine (Fluka Biochemika, Switzerland). U73122 was dissolved in IVDB at 2 mM and diluted to 10 μM in Krebs solution. Stock solutions of

nifedipine (10 mM) and nimodipine (20 mM) were dissolved in 100% ethanol and 2-APB (60 mM) in DMSO. Appropriate dilutions of ethanol and DMSO in Krebs solution showed no effects on either contractions or depolarizations. Pimozide and flunarizine were dissolved directly in Krebs solution. Other drugs were prepared as ×1000 stocks in distilled water and diluted in Krebs solution. Krebs solution containing 40 mM KCl was prepared by equimolar replacement of NaCl.

Analysis

Effect of drugs and current steps on resting vessel diameter (RVD), membrane potential and wall calcium was determined relative to values in control solution as previously.[12] Data were analysed with paired t-tests for single drugs and with one-way ANOVA followed by t-tests using Bonferroni correction for multiple drug exposure. Values are means ± S.E.M. of n preparations, each from a separate animal. Results were considered significant for $p<0.05$.

Messenger RNA extraction and RT-PCR

The pia was removed from the blood vessels which were placed in RNAlater (Ambion). Pooled arteries from 13-17 rats (n = 5 samples) were snap-frozen in liquid nitrogen, ground in a cold mortar and resuspended in 600 µL of lysis buffer + 1% β-mercaptoethanol. RNA was isolated using RNeasy minicolumns (Qiagen, USA), including DNase digestion (30 min).

Messenger RNA was reverse transcribed to cDNA (42°C 1h, 50°C 1h, 90°C 10 min) using oligo dT (500 ng/µL, Invitrogen, USA) primers and Superscript II (200 U/µL, Invitrogen). For each sample, reactions from which reverse transcriptase was omitted were run to control for contaminating DNA.

Primers were designed to be complementary to the published rat sequences for each of the pore-forming (α1) subunits of the VDCCs and to include as many known variants as possible. Table 2 contains primer sequences and product sizes. PCR conditions for each primer pair (Table 3) were determined using positive controls for each Ca_V subtype, i.e. brain cortex for $Ca_V1.2$,[38] $Ca_V1.3$,[38] $Ca_V2.2$,[2] $Ca_V2.3$,[2] $Ca_V3.1$,[2] and $Ca_V3.2$,[39] skeletal muscle for $Ca_V1.1$,[2] retina for $Ca_V1.4$,[2] cerebellum for $Ca_V2.1$,[40] and brain striatum for $Ca_V3.3$.[41] Reaction mixtures (20 µl) contained 500 nM of each primer (except 250 nM for $Ca_V2.2$) (Operon, USA), Taq polymerase (1 U/reaction), dNTPs (200 µM) and 50 ng cDNA template. Products were stained with ethidium bromide after electrophoresis of 2% agarose gels. Every experiment included control reactions which lacked cDNA or contained untranscribed RNA.

Quantitative PCR

The basilar artery was separated from its lateral branches before RNA extraction and reverse transcription. Quantitative PCR was used to determine the absolute copy numbers of VDCC subtypes using standard curves constructed by amplification of known quantities of plasmid DNA containing the cloned PCR products that were detected by semi-quantitative PCR, i.e. $Ca_V1.2$, $Ca_V1.3$, $Ca_V3.1$, $Ca_V3.2$, and $Ca_V2.3$. Cloned PCR products were confirmed by sequencing (ABI 3730 Capillary Genetic Analyser, ACRF Biomolecular Resource Facility, JCSMR, ANU).

PCR reaction mixtures (25 µL) were prepared using the SYBR Green Core Reagents Kit (Applied Biosystems) and contained 0.6 U of Amplitaq Gold, 800 nM of each primer, 1mM dNTPs, 1X SYBR Green buffer, 3mM $MgCl_2$ and 10 ng cDNA or 5 µL diluted plasmid containing the cloned insert of interest. Duplicate reactions were performed in the ABI Prism 7700 Sequence Detection System (Applied Biosystems) at 95°C for 12 min, 40 cycles of 95°C for 10 s, 67°C for 10s for $Ca_V3.1$, $Ca_V1.2$, $Ca_V1.3$, $Ca_V3.2$; 65°C for $Ca_V2.3$; and 61°C for 15s for 18S rRNA, followed by 72°C 60s.

The expression of all of the genes was determined in each of 3 samples with appropriate controls as described above. The integrity of each PCR reaction was checked using dissociation curve analysis after every reaction (95°C for 15 s, 60°C for 20 s and 95°C for 15 s).

The copy number in every sample was normalized to expression of 18S rRNA. Results were analyzed for statistical significance ($P < 0.05$) using one-way analysis of variance (ANOVA) and Student's t-test with Bonferroni correction for multiple comparisons. Expression of the same gene in the basilar artery and its branches was analysed using paired t-tests.

Cloning and sequencing of $Ca_V3.1$ and $Ca_V3.2$ domains I, II and I-II linker

Using primers designed to span domains I, II and I-II linker of $Ca_V3.1$ and $Ca_V3.2$ (Table 2), cDNA was amplified through PCR using 0.5 U/reaction of HotMaster Taq DNA Polymerase (Eppendorf, Germany) according to the following conditions: 95°C for 2 min, 40 cycles of 95°C for 10 s, 66°C for 10 s, 72°C for 80 s, final cycle of 72°C for 5 min. PCR products were visualized through agarose gel electrophoresis and ethidium bromide staining.

Single amplicons were purified directly from the PCR reaction mix. When multiple amplicons were present, the most strongly amplified bands were purified after electrophoresis, according to the manufacturer's instructions (QIAquick PCR Purification Kit (QIAGEN, USA). Purified PCR products were ligated into the pCR4-TOPO vector (Invitrogen) and plasmid DNA containing the cloned products isolated (QIAprep miniprep kit, Qiagen, USA).

Both strands of the cloned PCR products of domains I, II and I-II linker of $Ca_V3.1$ and $Ca_V3.2$ were sequenced on an ABI 3730 sequencer (ACRF Biomolecular Resource Facility). Nucleotide sequences were translated into protein using software provided by the Swiss Institute of Bioinformatics (http://au.expasy.org/tools/dna.html).[42] The nucleotide and amino acid sequences of cloned fragments were compared with all publicly available Ca_v sequences

Table 3. PCR conditions

Channel	Number of cycles	Annealing	Extension
$Ca_V1.1$	35	65°C 10 s	72°C 10 s
$Ca_V1.2$	35	67°C 5 s	72°C 10 s
$Ca_V1.3$	35	67°C 5 s	72°C 10 s
$Ca_V1.4$	36	67°C 10 s	72°C 10 s
$Ca_V2.1$	35	65°C 5 s	72°C 15 s
$Ca_V2.2$	35	67°C 5 s	72°C 10 s
$Ca_V2.3$	35	65°C 10 s	72°C 20 s
$Ca_V3.1$	35	67°C 5 s	72°C 15 s
$Ca_V3.2$	35	67°C 5 s	72°C 10 s
$Ca_V3.3$	35	67°C 10 s	72°C 10 s
$Ca_V3.1$ Domains I and II and I-II linker	40	66°C 10 s	72°C 80 s
$Ca_V3.2$ Domains I and II and I-II linker	40	66°C 10 s	72°C 80 s

using BLAST software and rat genome sequence data provided by GenBank (http://www.ncbi.nlm.nih.gov). Gene sequences have been deposited in the GenBank database (GenBank accession numbers EF116282, EF116283, EF116284, EF116285, EF116286, EF116287, EF116288, EU293201).

Immunohistochemistry

The basilar artery and side branches were processed as wholemounts and incubated overnight at 4°C in rabbit antibodies raised against peptides from $Ca_v3.1$ (FVCQGEDTRNITNKSDCAEAS) or $Ca_v3.2$ (YYCEGPDTRNISTKAQCRAAH),[43] diluted (1:300) in PBS containing 2% bovine serum albumin and 0.2% Triton X100. Similar incubations were made with commercial rabbit antibodies raised against $Ca_v3.1$ (1:100; Alomone Labs), $Ca_v3.2$ (1:100; Santa Cruz), $Ca_v1.2$, $Ca_v1.3$ and $Ca_v2.3$ (1:300; Alomone Labs). Staining was visualized after incubation for 3h in Cy3 conjugated anti-rabbit IgG (1:100, Jackson Immunoresearch Laboratories). Preparations were subsequently incubated briefly in 0.001% propidium iodide to label cell nuclei. Serial confocal images were taken of the Cy3 staining throughout the cell layers of wholemounts and selected sections recombined to visualise the smooth muscle. Specificity of the staining was tested by omission of the primary antibody or preincubation of the antibody with a ten-fold excess of the immunogenic peptide.

Results

Role of nifedipine-insensitive VDCCs in control of vascular tone

Following a 30 min incubation period, arteries typically exhibited spontaneous vasomotion which was preceded by oscillations in membrane potential and oscillations in the intracellular calcium concentration of individual smooth muscle cells. The L-type VDCC blocker, nifedipine (1 μM), abolished vasomotion (n = 18), oscillations in wall calcium (n = 8) and membrane potential (n = 10), without significantly affecting vascular tone (100.1 ± 0.6 % RVD in control; $P > 0.05$; paired t-test, n = 18; Table 4). Nifedipine produced depolarization (control: −45.1 ± 2.1 mV; nifedipine: −42.8 ± 2.3 mV; $P < 0.05$; paired t-test, n = 10), basal calcium levels increased (104.8 ± 1.4 % $F_{340/380}$ in control; $P < 0.05$; paired t-test, n = 8; Table 4) and oscillations in calcium in individual smooth muscle cells became asynchronous, as we have described previously.[12]

A supramaximal concentration of nifedipine (10 μM) produced an effect similar to that of the lower concentration of 1 μM, i.e. vasomotion was abolished, the RMP depolarized significantly (control: −46 ± 2.7 mV; nifedipine −35 ± 1.9 mV; n = 4; $P < 0.05$) but there was still no loss of vascular tone (96 ± 1.2 % RVD in control, n = 4; $P > 0.05$; Figure 1 A, B; Table 4). The subsequent addition of nimodipine (10 μM) significantly hyperpolarized (nimodipine: −58 ± 2.0 mV; n = 4; $P < 0.05$) and relaxed the arteries (108 ± 1.8 % RVD in control, n = 4; $P < 0.05$; Figure 1C; Table 4).

In contrast to the effect of nifedipine, application of small hyperpolarizing current steps (−0.1 to −0.5 nA) to short segments of basilar artery immediately abolished vasomotion ($P < 0.05$) and produced relaxation (104 ± 0.5 % RVD in control; $P < 0.05$; paired t-test, n = 20; Figure 2A, B). Relaxations were similar in amplitude irrespective of the size of the current steps (Figure 2A, B) and occurred even for hyperpolarizing steps that took the artery to values around the most negative potential observed during diameter and voltage oscillations (RMP in all experiments: −45.4 ± 0.7 mV; n = 61). Both vasomotion and tone were restored immediately following cessation of the current pulse (Figure 2A, B).

Relaxation was also observed during negative current steps in the presence of nifedipine (10 μM; 103 ± 0.3 % RVD in nifedipine; $P < 0.05$; paired t-test, n = 6; Figure 2C, D). Relaxation in the presence of nifedipine was not significantly different from that in the absence of nifedipine (compare Figure 2A, B with C, D, respectively; unpaired t-test; $P > 0.05$).

In some short arterial segments, which were not spontaneously active, application of positive current steps

Table 4. Effect of VDCC blockers on responses of the rat basilar artery

Drug	Vessel Tone	Vasomotion	Basal calcium	Membrane Potential
Nifedipine 1μM	No effect (18)	Abolished (18/18)	Increased (8)	Depolarized (10)
Nifedipine 10μM	No effect (4)	Abolished (4/4)	ND	Depolarized (4)
Nifedipine 10μM + Nimodipine 10μM	Relaxed (4)	Abolished (4/4)	ND	Hyperpolarized (4)
Mibefradil 1μM	Relaxed (13)	Abolished (13/13)	Decreased (5)	Hyperpolarized (5)
Pimozide 10μM	Relaxed (14)	Abolished (9/14)	Decreased (6)	Hyperpolarized (5)
Flunarizine 100μM	Relaxed (7)	Abolished (5/7)	Decreased (7)	ND
$NiCl_2$ 100μM	No effect (10)	Decreased frequency (10/10)	ND	No effect (6)

Number of experiments in parentheses
ND not determined

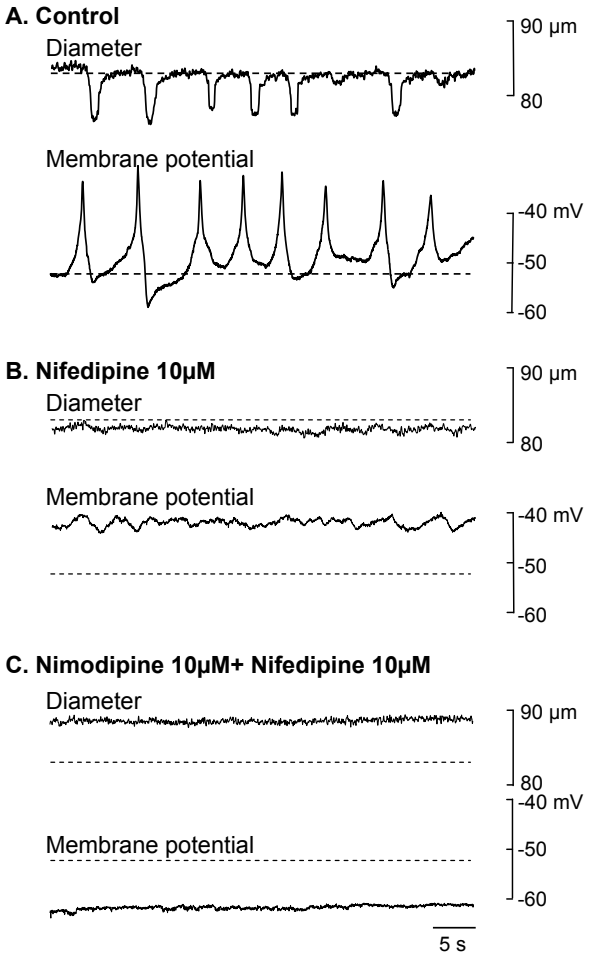

Figure 1. Effect of nimodipine on vasomotion, tone and membrane potential. *Application of a high concentration (10 μM) of nifedipine abolished vasomotion and membrane potential oscillations, depolarized the arteries but did not affect vascular tone (**A**, **B**). The addition of nimodipine (10 μM) to the Krebs solution containing nifedipine, hyperpolarized and relaxed the arteries (**C**). Dotted lines indicate comparable diameter and membrane potential levels in all traces.*

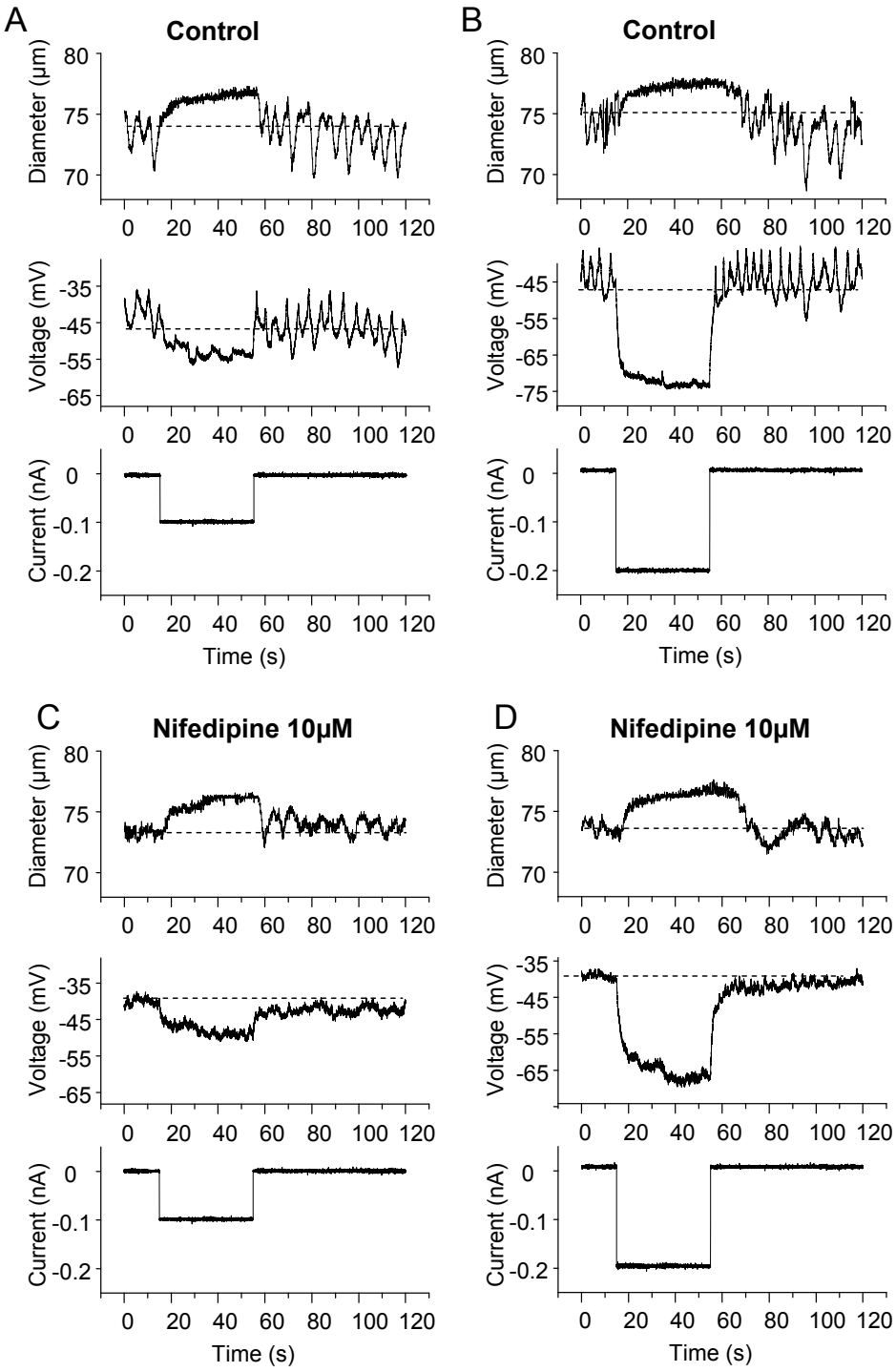

Figure 2. Hyperpolarization abolishes vasomotion and relaxes basilar artery segments. *Application of small hyperpolarizing currents to short segments of basilar arteries immediately abolished rhythmical depolarizations and contractions and relaxed the arteries (**A**, **B**). Tone and oscillations were re-gained immediately after the current application was stopped. Relaxation was similar in amplitude irrespective of the size of the current steps (**A**, **B**). Application of hyperpolarizing current steps relaxed the arterial segments even in the presence of the L-type VDCC blocker nifedipine (**C**, **D**). Dotted lines indicate resting vessel diameter or approximate resting membrane potential.*

(+0.05 to +0.5 nA) evoked depolarizations which, if large enough, were associated with vasoconstriction (9.0 ± 1.9 % RVD, n=3) and vasomotion (Figure 3A, B). After application of nifedipine (10 μM), vasoconstriction was still observed throughout the current pulse and this was not significantly different from that in control solution (9.2 ± 3.4 % RVD, n=3; P > 0.05, paired t-test). In contrast, vasomotion was not observed under these conditions (Figure 3C, D).

In order to determine the threshold for

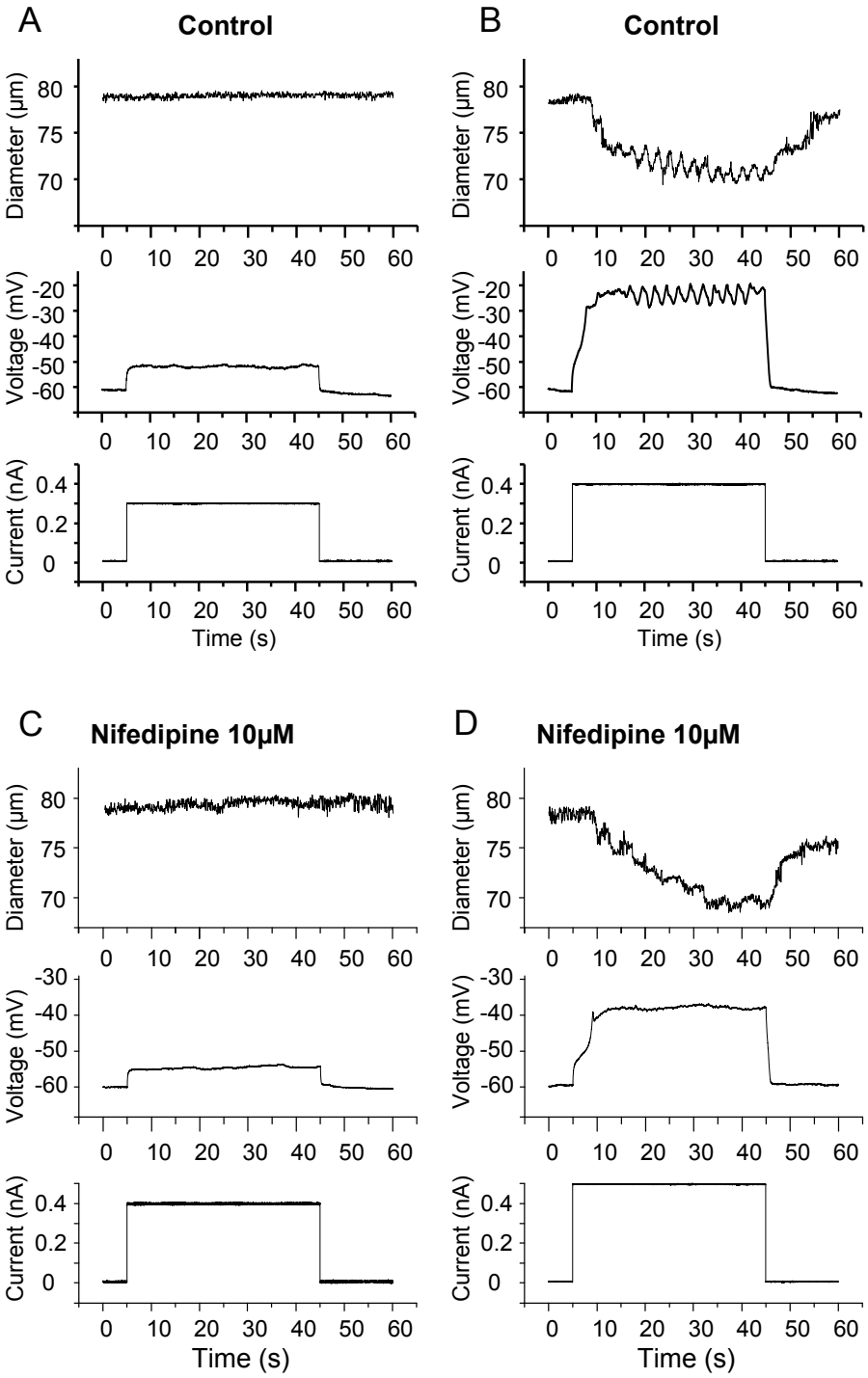

Figure 3. Depolarization induces vasoconstriction of basilar artery segments. *Application of depolarizing currents steps to short segments of quiescent basilar arteries evoked vasoconstriction and vasomotion (**A**, **B**). In the presence of the L-type VDCC blocker nifedipine, depolarizing current steps evoked vasoconstriction but not vasomotion (**C**, **D**).*

vasoconstriction in the presence of nifedipine, arteries were depolarized slowly with 40 mM KCl. In these experiments, vessels were relaxed and hyperpolarized by blocking the phospholipase C pathway with U73122 (10 μM).[12] Application of 40 mM KCl Krebs evoked a slow membrane depolarization to −30 ± 3.4 mV (n = 6), and a rise in wall calcium concentration (117 ± 1.2 % $F_{340/380}$ in U73122 + nifedipine; $P < 0.05$, n = 4). The membrane potential at which constriction was initiated in the presence of nifedipine was −40 ± 1.8 mV (n = 6).

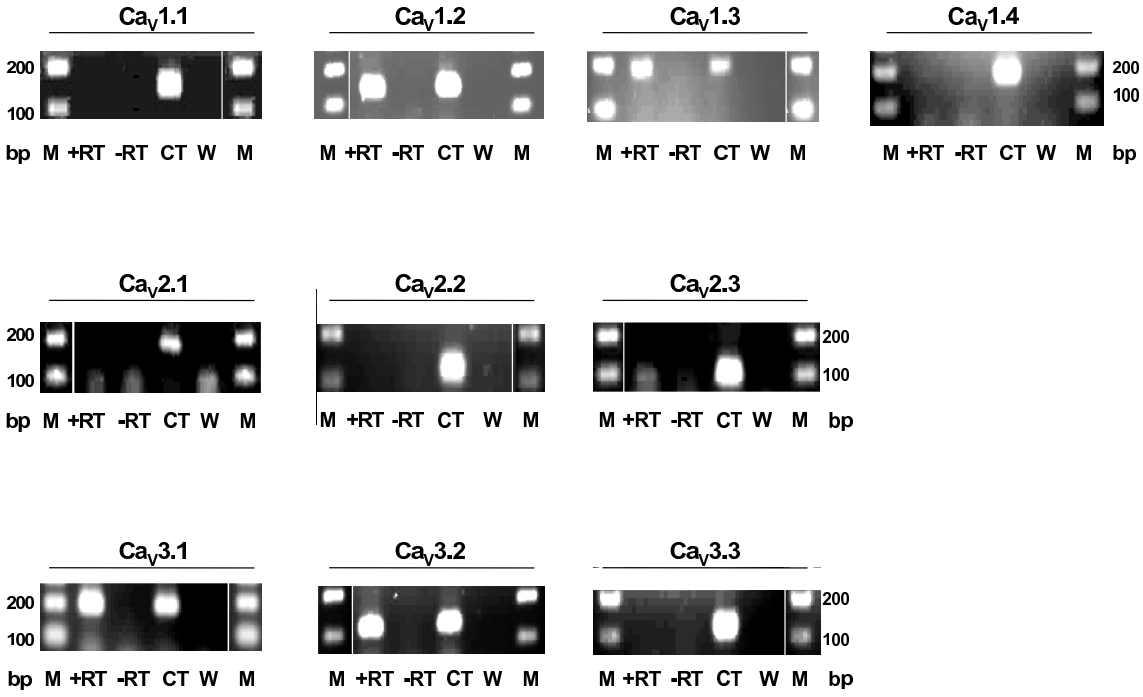

Figure 4. mRNA expression of VDCC subtypes in the basilar artery. *$Ca_V1.2$, $Ca_V1.3$, $Ca_V3.1$ and $Ca_V3.2$ were strongly expressed in the basilar artery. $Ca_V2.3$ was weakly expressed. Lanes: +RT, basilar artery containing RNA and Superscript II; −RT, basilar artery containing RNA but no Superscript II; CT, positive control; W, control PCR without cDNA. Rat brain cortex was used as positive control for the PCR reactions for $Ca_V1.2$, $Ca_V1.3$, $Ca_V2.2$, $Ca_V2.3$, $Ca_V3.1$ and $Ca_V3.2$, skeletal muscle for $Ca_V1.1$; retina for $Ca_V1.4$; cerebellum for $Ca_V2.1$; brain striatum for $Ca_V3.3$.*

Together these data demonstrate that both vascular tone and vasomotion are voltage dependent processes, but only vasomotion, and not vascular tone, depends on calcium influx through L-type VDCCs. In contrast to the selective L-type VDCC blocker, nifedipine, the dihydropyridine, nimodipine, produced effects on both vasomotion and vascular tone.

mRNA expression of VDCC subtypes in the basilar artery and branches

Strong mRNA expression for $Ca_V1.2$ (n=3), $Ca_V1.3$ (n=3), $Ca_V3.1$ (n=3), and $Ca_V3.2$ (n=3) was detected in basilar artery preparations, while $Ca_V2.3$ (n=5) was weakly expressed (Figure 4). $Ca_V1.1$, $Ca_V1.4$ (n = 3), $Ca_V2.1$, $Ca_V2.2$ (n = 4) and $Ca_V3.3$ (n = 3) were strongly expressed in rat skeletal muscle, retina, cerebellum, brain cortex and striatum, respectively, but were absent from the basilar artery (Figure 4).

Quantitative PCR showed that the order of expression was $Ca_V3.1$>$Ca_V1.2$>$Ca_V1.3$>$Ca_V3.2$>$Ca_V2.3$ in both the main and in the lateral branches (Table 5). Expression of $Ca_V3.1$ was significantly higher than that of the other 4 channels in both the main basilar artery and in the side branches. All of the channels tended to be more highly expressed in the lateral branches than in the main basilar artery, although this difference did not reach statistical significance.

Table 5. Expression of mRNA for Ca_V subtypes in the main basilar artery and branches.

Ca_V subtype	Basilar Artery	Lateral Branches
$Ca_V1.2$	1086 ±157 (3) *	3550 ± 1541 (3) *
$Ca_V1.3$	475 ± 79 (3) *	679 ± 478 (3) *
$Ca_V2.3$	45 ± 10 (3) *	48 ± 33 (3) *
$Ca_V3.1$	10730 ± 329 (3)	14820 ± 4895 (3)
$Ca_V3.2$	139 ± 33 (3) *	367 ± 113 (3) *

*Copy numbers for each subtype are expressed per 10^6 copies of 18S rRNA. Values are mean ± S.E.M. with number of samples in parentheses. * indicates significant difference from corresponding $Ca_V3.1$ expression in corresponding vessel.*

Protein expression of VDCC subtypes in the basilar artery and branches

Strong staining for $Ca_v3.1$ was found intracellularly adjacent to the nucleus and in the cell membranes of the smooth muscle cells of the basilar artery and its smaller side branches (Figure 5A). Clear punctate staining for $Ca_v1.2$ was also found in the smooth muscle cell membranes (Figure 5C). Weak immunoreactivity could be detected for $Ca_v3.2$ (Figure 5E), while no staining was found for $Ca_v1.3$ (data not shown). In the case of $Ca_v2.3$, the staining was confined to the very outer limit of the

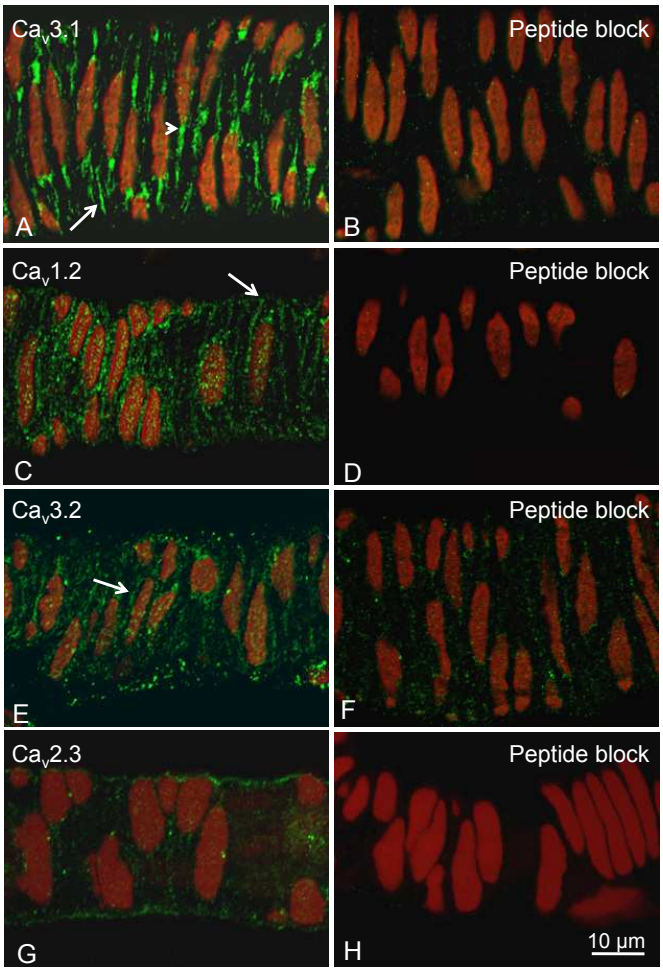

Figure 5. Protein expression of VDCC subtypes in the basilar artery. *Strong staining for $Ca_V3.1$ was found intracellularly near the nucleus (arrowhead) and in the cell membrane (white arrow) of the smooth muscle cells of the basilar artery branches (A). Punctate staining was also found in the cell membrane for $Ca_V1.2$ (white arrow, **C**). Weaker staining for $Ca_V3.2$ (**E**) could be detected (white arrows). Staining for $Ca_V2.3$ appeared to be confined to the outer limits of the vessel (**G**). Staining for all antibodies was abolished or greatly reduced by preincubation in the appropriate antigenic peptide (**B**, **D**, **F**, **H**). Transversely oriented smooth muscle cells were identified by nuclear staining with propidium iodide.*

vessel and was therefore not considered to be expressed in the smooth muscle (Figure 5G). Staining was abolished following incubation of the antibodies against $Ca_V3.1$, $Ca_V1.2$ and $Ca_V2.3$ with the appropriate antigenic peptide (Figure 5B, D, H) and greatly reduced for the antibodies against $Ca_V3.2$ (Figure 5F). Similar results were obtained for the 2 different antibodies directed against $Ca_V3.1$ and $Ca_V3.2$. These data showed that the L- and T-type VDCCs, $Ca_V1.2$ and $Ca_V3.1$, were the most strongly expressed subtypes in the smooth muscle cells of the basilar artery and branches.

Role of T-type VDCCs in control of vascular tone

Application of the T-type VDCC blocker mibefradil (1µM) abolished vasomotion (n = 13) and relaxed branches of the basilar artery (121 ± 3.4 % RVD in control; $P < 0.05$; paired t-test, n = 13; Figure 6A; Table 4). Mibefradil decreased wall calcium levels (79 ± 6.5 % $F_{340/380}$ in control; $P < 0.05$; paired t-test, n = 5; not shown), abolished calcium oscillations in smooth muscle cells (n = 3) and hyperpolarized the cell membrane (control: −40 ± 0.4 mV; mibefradil: −60 ± 3.7 mV; $P < 0.05$; paired t-test, n = 5; Figure 6A).

The T-type VDCC blocker pimozide (10 µM) also relaxed (109 ± 1.8 % RVD in control; $P < 0.05$; paired t-test, n = 14), and hyperpolarized basilar arteries (control: −43 ± 2.8 mV; pimozide: −56 ± 2.6 mV; $P < 0.05$; paired t-test, n = 5; Figure 6B; Table 4), decreased basal calcium (94 ± 1.7 % $F_{340/380}$ in control; $P < 0.05$; paired t-test, n = 6), and decreased the frequency of contractions (control: 15.8 ± 1.1 contractions per minute; pimozide: 4.8 ± 2.1 contractions per minute; $P < 0.05$; paired t-test, n = 14). In 9 of 14 experiments vasomotion was completely abolished, and in 4 of 6 experiments measuring calcium, oscillations in individual smooth muscle cells were abolished.

Incubation with the T-type VDCC blocker flunarizine (100 µM) produced relaxation (106 ± 1.1 % RVD in control; $P < 0.05$; paired t-test, n = 7), significantly decreased basal calcium levels (94 ± 1.7 % $F_{340/380}$ in control; $P < 0.05$; paired t-test, n = 7) and the frequency of vasomotion (control: 13.7 ± 1.4 contractions per minute; flunarizine: 1.3 ± 0.9 contractions per minute; $P < 0.05$; paired t-test, n = 7; Table 4). In 5 out of 7 experiments vasomotion was completely abolished.

Since $Ca_V3.1$ and $Ca_V3.2$ VDCCs were both expressed in the basilar microcirculation, low concentrations of $NiCl_2$ (100µM) were used to differentiate between their actions, since the IC_{50} for $Ca_V3.2$ channels is 13 µM while the IC_{50} for $Ca_V3.1$ is 250 µM.[37] At this concentration, there was no significant effect on arterial tone (102 ± 1.9 % RVD in control; $P > 0.05$; n = 10) or membrane potential (control: −49 ± 2.2 mV; n = 6; 100 µM $NiCl_2$: −47 ± 3.9 mV; n = 6; $P > 0.05$), although the frequency of vasomotion was reduced (frequency control: 16.6 ± 0.8 oscillations per minute; n = 10; 100 µM $NiCl_2$: 8.0 ± 1.9 oscillations per minute; n = 10; $P < 0.05$; Table 4), suggesting that $Ca_V3.2$ VDCCs were not involved. A higher, non-selective concentration of nickel chloride (1 mM) abolished vasomotion ($P < 0.05$; n = 7) and relaxed arteries (108 ± 2.8 % RVD in control; $P < 0.05$; n = 7), showing a trend towards hyperpolarization (control: −49 ± 2.2 mV; n = 6; 1 mM $NiCl_2$: −55 ± 5.9 mV; n = 3; $P > 0.05$; unpaired t-test).

Taken together, the results demonstrate a role for T-type VDCCs, of the $Ca_V3.1$ subtype, in providing the calcium influx necessary for the maintenance of vascular tone in the rat basilar artery.

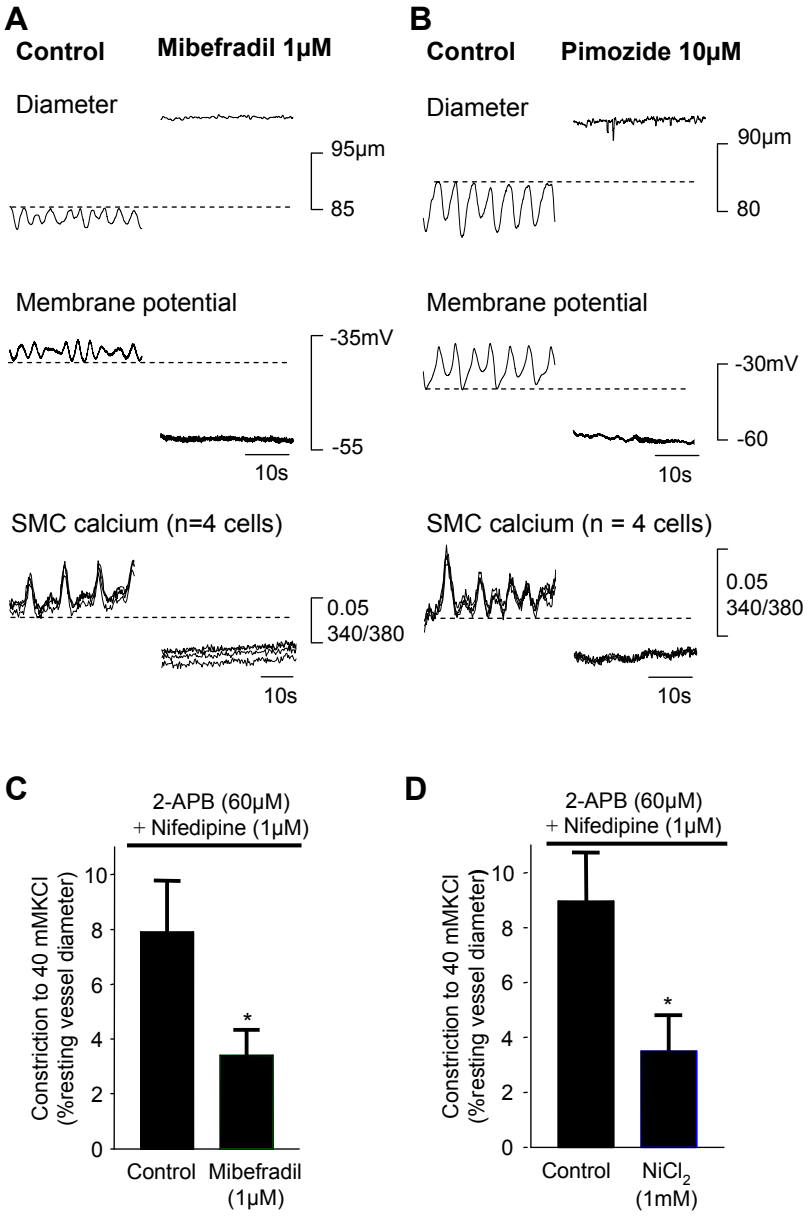

Figure 6. Effect of T- type VDCC blockers on tone, membrane potential and [Ca]$_i$. *Application of mibefradil (1 μM, **A**) and pimozide (10 μM, **B**) abolished vasomotion, relaxed and hyperpolarized basilar arteries, abolished oscillations of calcium in individual smooth muscle cells and decreased basal calcium levels. **C**. After arteries had been relaxed with 2-APB (60 μM) and L-type VDCCs had been blocked with nifedipine (1 μM), application of 40 mM KCl produced constriction of basilar arteries (control). This contraction was significantly reduced by mibefradil (1 μM). **D**. Constriction evoked by 40 mM KCl was similarly attenuated by a high, non-selective concentration of nickel chloride (1 mM).*
** P < 0.05 significantly different from the corresponding control.*

Role of T-type channels in vasoconstriction evoked by depolarization

In these experiments, arteries were relaxed by inhibiting IP_3 receptors with 2-APB (60 μM[44]) or by blocking the phospholipase C pathway with U73122 (10 μM). In the presence of nifedipine (1 μM) to block L-type channels, 2-APB relaxed the arteries (106 ± 1.6 % RVD in control, P < 0.05). Subsequent application of Krebs solution containing 40 mM KCl, in the continued presence of 2-APB and nifedipine, produced vasoconstriction which was significantly reduced by mibefradil (1 μM; Control: 7.9 ± 1.9 % RVD in 2-APB and nifedipine; mibefradil: 3.4 ± 0.9 % RVD in 2-APB and nifedipine; P < 0.05, n = 4; Figure 6C) or a non specific concentration of nickel chloride (1mM; Control: 9.0 ± 1.8 % RVD in 2-APB and nifedipine; $NiCl_2$: 3.5 ± 1.3 % RVD in 2-APB and nifedipine; P < 0.05, n = 5; Figure 6D). After relaxation with U73122, in the presence of nifedipine, 40 mM KCl evoked vasoconstriction (15 ± 3.5 % RVD, n = 7), which

was also significantly reduced following incubation in mibefradil (1 μM; 9 ± 3.3 % RVD in U73122, nifedipine and mibefradil; $P < 0.05$; $n = 7$).

These data suggest that vasoconstriction evoked by depolarization results from calcium influx through nifedipine-insensitive VDCCs.

Sequencing of T-type channels

In order to identify whether the T-type VDCCs expressed in the basilar artery were typical $Ca_V3.1$ and $Ca_V3.2$ channels, we cloned and sequenced domains I, II and the I-II linker regions. The location of the primers in the $Ca_V3.1$ sequence is shown in Figure 7. Primers used for $Ca_V3.2$ were located in similar regions.

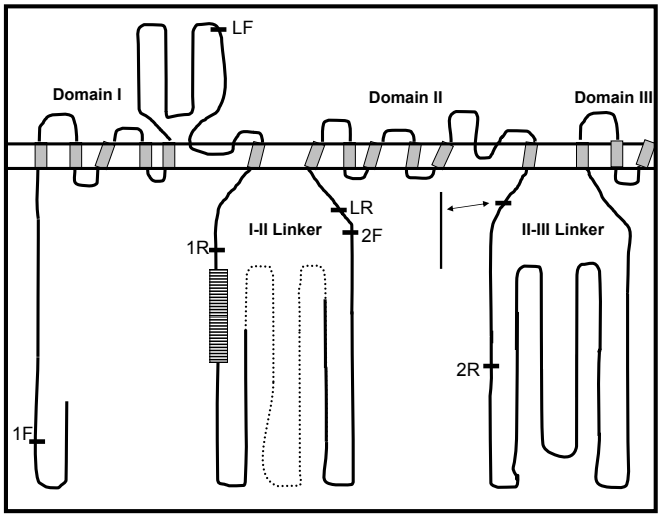

Figure 7. Schematic representation of the aminoacid structure of $Ca_V3.1$. *1F and 1R denote location of forward and reverse primers, respectively, against domain I. LF and LR denote location of forward and reverse primers, respectively, against I-II Linker. 2F and 2R denote location of forward and reverse primers, respectively, against domain II. Rectangle with horizontal lines represents location of alpha interaction domain in high voltage activated calcium channels. Dotted line represents the approximate location and size of deletion in novel splice variant. Double-ended arrow represents approximate size (left) and location (right) of insertion in splice variant. Domain IV not shown. Modified from Perez-Reyes, 2003, Physiol. Rev. 83:117-61.*

Sequencing of domain I of $Ca_V3.1$ revealed the expected 1215 bp fragment, including the last 63 amino acids of the N-terminus and the first 27 amino acids of the I-II linker. This showed 100% homology with $Ca_V3.1$ sequences, GenBank accession numbers AF125161 and AF290212.

PCR of the I-II linker of $Ca_V3.1$, from 27 amino acids before the intramembrane portion between IS5 and IS6 to 12 amino acids before the beginning of domain II revealed 2 main fragments of 1269 bp (expected) and 867 bp which were sequenced. The 1269 bp fragment was 100% homologous with sequences, GenBank accession numbers AF125161 and AF290212. The 867 bp sequence was 100% homologous with $Ca_V3.1$ sequences, GenBank accession numbers AF125161 and AF290212, except that it lacked the last 402 nucleotides of exon 9. This exclusion encodes 134 amino acids, beginning 114 amino acids into the I-II linker (Figure 7, dotted region).

PCR of domain II of $Ca_V3.1$ from the last 17 amino acids of the I-II linker to the start of the II-III linker revealed 2 bands of 856 bp and 925 bp. Sequencing showed that the 856 bp band was 100% homologous with GenBank accession number AF290212, while the 925 bp band was 100% homologous with GenBank accession number AF125161, isolated from insulin-secreting cells. The 856 bp sequence lacks exon 15, which is present in the 925 bp band. This exon encodes for 23 amino acids beginning 6 amino acids into the II-III linker (see double ended arrow indicating insertion in Figure 7).

PCR of domains I, II and the I-II linker of $Ca_V3.2$ revealed bands with the expected sizes of 1267 bp, 1014 bp, and 1069 bp, respectively, and were homologous with the $Ca_V3.2$ sequence, GenBank accession no AF290213.

Discussion

The present study has shown a differential involvement of VDCC subtypes in cerebrovascular function; L-type VDCCs were essential for vasomotion, while non-L-type VDCCs, with pharmacology matching that of T-type channels, controlled vascular tone. Consistent with this physiological data, real-time PCR and immunohistochemistry demonstrated expression of both L- and T-type channels, with the most highly expressed subtypes in both the main basilar artery and its smaller side branches being the $Ca_v1.2$ and $Ca_v3.1$. Since the membrane potential of the smooth muscle cells of the rat basilar artery in the present study was around −45mV, a value similar to that of cerebral arteries subjected to intraluminal pressure,[45,46] we conclude that the T-type channels expressed in these vessels must be activated and inactivated at more depolarized potentials, similar to the T-type channels identified in other blood vessels.[1]

While incubation in the L-type VDCC antagonist, nifedipine, abolished vasomotion, it had no effect on vascular tone of rat basilar arteries.[12] In contrast, injection of small hyperpolarizing current steps into short arterial segments in the presence of supramaximal concentrations of nifedipine produced immediate relaxation and loss of vasomotion, suggesting that non L-type VDCCs control vascular tone. In a comparable fashion, depolarization of quiescent arteries led to vasoconstriction, despite the presence of nifedipine, but did not produce vasomotion. Taken together, the results support the conclusion that L-type VDCCs are essential for vasomotion but non L-type channels are instrumental in determining vascular tone in these cerebral arteries.

Support for a role of non L-type VDCCs came from our quantitative PCR studies which revealed strong

expression of two L-type ($Ca_V1.2$ and $Ca_V1.3$) and two T-type ($Ca_V3.1$ and $Ca_V3.2$) VDCC channels in the rat basilar artery and its branches, with similar relative mRNA expression showing $Ca_V3.1 > Ca_V1.2 > Ca_V1.3 > Ca_V3.2 > Ca_V2.3$. At the protein level, $Ca_V3.1$ and $Ca_V1.2$ were both clearly expressed in the vascular smooth muscle cells, while much lower levels of $Ca_V3.2$ were found, $Ca_V1.3$ was not detected and $Ca_V2.3$ was confined to the surface of the vessel. We found no evidence for expression of N-type channels ($Ca_V2.2$) as described in the dog basilar artery,[17] or of P/Q-type channels ($Ca_V2.1$) as found in rat renal arterioles[47,48] suggesting that further variation may occur between vascular beds and species.

While nifedipine had no effect on basilar tone, the subsequent addition of nimodipine evoked relaxation and hyperpolarization, suggesting a non-specific action on other VDCCs, as previously described.[23-26] Three putative T-type channel antagonists, mibefradil, pimozide and flunarizine, produced a similar effect on membrane potential and vascular tone. In the absence of significant expression of other high voltage activated VDCCs, the data support a role for T-type channels in this vessel. Since $Ca_V3.2$ VDCCs are more sensitive to nickel chloride than are $Ca_V3.1$ VDCCs,[37] we tested low concentrations of nickel chloride but found no effect on either vascular tone or membrane potential. We therefore propose that vascular tone in the rat basilar artery and its microcirculation is provided by influx of calcium through nifedipine-insensitive VDCCs with pharmacology matching that of T-type $Ca_V3.1$ channels.

We found that depolarization-induced vasoconstriction produced by 40mM KCl, in the presence of L-type channel blockade, was initiated at a membrane potential of −40 mV. Furthermore, this depolarization-induced constriction was significantly reduced by mibefradil in the continued presence of dihydropyridines. Although classical T-type channels would be expected to be closed at these potentials,[1] T-type channels exhibiting a maximal window current around −37mV have been characterized in smooth muscle cells of the dog basilar artery, along with mRNA and protein for $Ca_V3.1$ and $Ca_V3.3$.[17] Such channels could therefore contribute to cerebrovascular tone as they would be open at physiologically relevant membrane potentials. Indeed, the T-type currents found in the dog basilar artery were inhibited by nimodipine and mibefradil which also produced relaxation of arterial segments.[17] Whether T-type channels are expressed and are functional in other parts of the cerebral circulation remains to be determined.

A nifedipine-insensitive VDCC with high voltage activation and possessing pharmacological properties resembling T-type channels has been described in terminal mesenteric arterioles.[25,26,49-51] While the expression of T-type channels was not investigated in these studies,[25,26] others have shown that small mesenteric arterioles of <40 μm express T-, but not L-type, channels which are responsible for local and conducted vasoconstriction and depolarization-induced calcium influx.[52,53] It seems unlikely, however, that these peripherally located T-type channels in the microcirculation are responsible for systemic blood pressure regulation since conditional knockout of $Ca_V1.2$ with the Cre/lox site specific recombination system, and tamoxifen as the inducer, produced a severe reduction in blood pressure and depolarization-induced constriction was absent in resistance sized (100-150 μm) skeletal muscle arteries.[54] Nevertheless, T-type VDCCs have also been implicated in the function of the renal microcirculation and a role in renal injury has been proposed.[55,56]

Cloning and sequencing of domains I to II of $Ca_V3.1$ and $Ca_V3.2$ failed to identify any alterations to transmembrane segments, defined in previous mutagenesis studies,[57] that could account for a shift in voltage dependence of activation towards more depolarized potentials. Indeed, in the case of $Ca_V3.2$, the entire region encompassing domains I, II and the I-II linker was identical to the sequences available in international databases. In contrast, sequencing of $Ca_V3.1$ demonstrated expression of 2 splice variants in the linker regions. One was an insertion in the II-III linker, previously described in $Ca_V3.1$ channels isolated from insulin-secreting cells,[58] while the other was a novel deletion in the I-II linker.

The I-II linker has been shown to be important for the binding of auxiliary subunits in high voltage activated channels[30] and for modulation of surface expression.[31] However, the absence of any modification to the region in the I-II linker corresponding to the alpha interaction domain in high voltage activated channels suggests that the channels expressed in the basilar artery are no more regulated by auxiliary subunits than are normal T-type channels.[59] In contrast, the novel deletion in the I-II linker of $Ca_V3.1$ spans a 402 bp segment encoding 134 amino acids located in a region homologous to that shown recently to modulate surface expression of $Ca_V3.2$ channels.[31] Whether expression of this novel splice variant results in increased surface expression and hence the size of the window current of the $Ca_V3.1$ channels is yet to be determined.

The insertion of 23 amino acids encoded by exon 15 after the end of domain II of $Ca_V3.1$ was identical to a splice variant isolated from insulin-secreting cells.[58] Interestingly, this channel has higher voltage activation and window current than other T-type channels[58] and could therefore contribute to the properties found in the present study. Amplification of cDNA from the end of domain I to the end of domain II indicates that these two splice variants may occur in the same and separate transcripts (unpublished observations). Future studies are required to determine the relative protein expression and properties of these splice variants.

We conclude that non L-type VDCCs are responsible for the maintenance of vascular tone of the rat basilar artery by providing a persistent inward current at physiological membrane potentials. Our molecular and immunohistochemical data indicate that L- and T-type channels are the predominant VDCCs expressed in this vessel and our pharmacological data support the involvement of $Ca_V3.1$. Cloning studies have shown that some of the $Ca_V3.1$ channels may contain splice variations

which may modify their properties or expression. T-type channels may therefore provide a potential target for therapeutic control of cerebrovascular tone during vasospastic conditions.

Acknowledgements

Work was supported by International and ANU Postgraduate Research Scholarships to MN-G and project grants from the National Health and Medical Research Council (471420) and Australian Research Council (DP0663818) to CEH.

References

1. Perez-Reyes E. Molecular physiology of low-voltage-activated t-type calcium channels. *Physiol. Rev.* 2003; **83:** 117-61.
2. Lacinová L. Voltage-dependent calcium channels. *Gen. Physiol. Biophys.* 2005; **24 Suppl 1:** 1-78.
3. Gerthoffer WT, Shafer PG, Taylor S. Selectivity of phenytoin and dihydropyridine calcium channel blockers for relaxation of the basilar artery. *J. Cardiovasc. Pharmacol.* 1987; **10:** 9-15.
4. Usui H, Akimoto Y, Kurahashi K, *et al.* Effects of nitroglycerin on stable thromboxane A2 analogue-induced, nifedipine-resistant contraction in canine basilar artery. *Jpn. J. Pharmacol.* 1990; **54:** 237-40.
5. Varsos VG, Liszczak TM, Han DH, *et al.* Delayed cerebral vasospasm is not reversible by aminophylline, nifedipine, or papaverine in a "two-hemorrhage" canine model. *J. Neurosurg.* 1983; **58:** 11-7.
6. Katori E, Ohta T, Nakazato Y, Ito S. Vasopressin-induced contraction in the rat basilar artery in vitro. *Eur. J. Pharmacol.* 2001; **416:** 113-21.
7. Teixeira CE, Priviero FB, Todd J, Jr., Webb RC. Vasorelaxing effect of BAY 41-2272 in rat basilar artery: involvement of cGMP-dependent and independent mechanisms. *Hypertension* 2006; **47:** 596-602.
8. Nakayama K. Calcium-dependent contractile activation of cerebral artery produced by quick stretch. *Am. J. Physiol.* 1982; **242:** H760-8.
9. Hogestatt ED, Andersson KE, Edvinsson L. Effects of nifedipine on potassium-induced contraction and noradrenaline release in cerebral and extracranial arteries from rabbit. *Acta Physiol. Scand.* 1982; **114:** 283-96.
10. Asano M, Aoki K, Suzuki Y, Matsuda T. Effects of Bay k 8644 and nifedipine on isolated dog cerebral, coronary and mesenteric arteries. *J. Pharmacol. Exp. Ther.* 1987; **243:** 646-56.
11. Omote M, Mizusawa H. Interaction between the L-type Ca^{2+} channel and the Ca^{2+}-activated K^+ channel in the fluctuating myogenic contraction in the rabbit basilar artery. *Jpn. J. Physiol.* 1996; **46:** 353-6.
12. Haddock RE, Hill CE. Differential activation of ion channels by inositol 1,4,5-trisphosphate (IP_3)- and ryanodine-sensitive calcium stores in rat basilar artery vasomotion. *J. Physiol.* 2002; **545:** 615-27.
13. Alborch E, Salom JB, Perales AJ, *et al.* Comparison of the anticonstrictor action of dihydropyridines (nimodipine and nicardipine) and Mg^{2+} in isolated human cerebral arteries. *Eur. J. Pharmacol.* 1992; **229:** 83-9.
14. Forsman M, Fleischer JE, Milde JH, Steen PA, Michenfelder JD. The effects of nimodipine on cerebral blood flow and metabolism. *J. Cereb. Blood Flow Metab.* 1986; **6:** 763-7.
15. Fujii K, Heistad DD, Faraci FM. Ionic mechanisms in spontaneous vasomotion of the rat basilar artery *in vivo*. *J. Physiol.* 1990; **430:** 389-98.
16. Muller-Schweinitzer E, Neumann P. In vitro effects of calcium antagonists PN 200-110, nifedipine, and nimodipine on human and canine cerebral arteries. *J. Cereb. Blood Flow Metab.* 1983; **3:** 354-61.
17. Nikitina E, Zhang ZD, Kawashima A, *et al.* Voltage-dependent calcium channels of dog basilar artery. *J. Physiol.* 2007; **580:** 523-41.
18. Peroutka SJ, Banghart SB, Allen GS. Relative potency and selectivity of calcium antagonists used in the treatment of migraine. *Headache* 1984; **24:** 55-8.
19. Towart R. The selective inhibition of serotonin-induced contractions of rabbit cerebral vascular smooth muscle by calcium-antagonistic dihydropyridines. An investigation of the mechanism of action of nimodipine. *Circ. Res.* 1981; **48:** 650-7.
20. Tsuji T, Cook DA. Effect of nimodipine on canine cerebrovascular responses to 5-hydroxytryptamine and potassium chloride after exposure to blood. *Stroke* 1989; **20:** 105-11.
21. White RP, Cunningham MP, Robertson JT. Effect of the calcium antagonist nimodipine on contractile responses of isolated canine basilar arteries induced by serotonin, prostaglandin F2a, thrombin, and whole blood. *Neurosurgery* 1982; **10:** 344-8.
22. Alborch E, Salom JB, Torregrosa G. Calcium channels in cerebral arteries. *Pharmacol. Ther.* 1995; **68:** 1-34.
23. Heady TN, Gomora JC, Macdonald TL, Perez-Reyes E. Molecular pharmacology of T-type Ca^{2+} channels. *Jpn. J. Pharmacol.* 2001; **85:** 339-50.
24. Randall AD, Tsien RW. Contrasting biophysical and pharmacological properties of T-type and R-type calcium channels. *Neuropharmacology* 1997; **36:** 879-93.
25. Morita H, Cousins H, Onoue H, Ito Y, Inoue R. Predominant distribution of nifedipine-insensitive, high voltage-activated Ca^{2+} channels in the terminal mesenteric artery of guinea pig. *Circ. Res.* 1999; **85:** 596-605.
26. Morita H, Shi J, Ito Y, Inoue R. T-channel-like pharmacological properties of high voltage-activated, nifedipine-insensitive Ca^{2+} currents in the rat terminal mesenteric artery. *Br. J. Pharmacol.* 2002; **137:** 467-76.
27. Mecca TE, Love SD. Comparative cardiovascular actions of clentiazem, diltiazem, verapamil,

nifedipine, and nimodipine in isolated rabbit tissues. *J. Cardiovasc. Pharmacol.* 1992; **20:** 678-82.
28. Zuccarello M, Boccaletti R, Tosun M, Rapoport RM. Role of extracellular Ca^{2+} in subarachnoid hemorrhage-induced spasm of the rabbit basilar artery. *Stroke* 1996; **27:** 1896-902.
29. Firat MM, Gelebek V, Orer HS, Belen D, Firat AK, Balkanci F. Selective intraarterial nimodipine treatment in an experimental subarachnoid hemorrhage model. *AJNR Am. J. Neuroradiol.* 2005; **26:** 1357-62.
30. Arias JM, Murbartian J, Vitko I, Lee JH, Perez-Reyes E. Transfer of b-subunit regulation from high to low voltage-gated Ca^{2+} channels. *FEBS Lett.* 2005; **579:** 3907-12.
31. Vitko I, Bidaud I, Arias JM, Mezghrani A, Lory P, Perez-Reyes E. The I-II loop controls plasma membrane expression and gating of Cav3.2 T-type Ca^{2+} channels: a paradigm for childhood absence epilepsy mutations. *J. Neurosci.* 2007; **27:** 322-30.
32. Neild TO. Measurement of arteriole diameter changes by analysis of television images. *Blood Vessels* 1989;26:48-52.
33. Mishra SK, Hermsmeyer K. Selective inhibition of T-type Ca^{2+} channels by Ro 40-5967. *Circ. Res.* 1994; **75:** 144-8.
34. McDonough SI, Bean BP. Mibefradil inhibition of T-type calcium channels in cerebellar purkinje neurons. *Mol. Pharmacol.* 1998; **54:** 1080-7.
35. Feng MG, Navar LG. Angiotensin II-mediated constriction of afferent and efferent arterioles involves T-type Ca^{2+} channel activation. *Am. J. Nephrol.* 2004; **24:** 641-8.
36. Santi CM, Cayabyab FS, Sutton KG, *et al.* Differential inhibition of T-type calcium channels by neuroleptics. *J. Neurosci.* 2002; **22:** 396-403.
37. Lee JH, Gomora JC, Cribbs LL, Perez-Reyes E. Nickel block of three cloned T-type calcium channels: low concentrations selectively block α_{1H}. *Biophys. J.* 1999; **77:** 3034-42.
38. Trimmer JS, Rhodes KJ. Localization of voltage-gated ion channels in mammalian brain. *Annu. Rev. Physiol.* 2004; **66:** 477-519.
39. Talley EM, Cribbs LL, Lee JH, Daud A, Perez-Reyes E, Bayliss DA. Differential distribution of three members of a gene family encoding low voltage-activated (T-type) calcium channels. *J. Neurosci.* 1999; **19:** 1895-911.
40. Lau FC, Abbott LC, Rhyu IJ, Kim DS, Chin H. Expression of calcium channel α_{1A} mRNA and protein in the leaner mouse (tgla/tgla) cerebellum. *Brain Res. Mol. Brain. Res.* 1998; **59:** 93-9.
41. McRory JE, Santi CM, Hamming KS, *et al.* Molecular and functional characterization of a family of rat brain T-type calcium channels. *J. Biol. Chem.* 2001; **276:** 3999-4011.
42. Gasteiger E, Gattiker A, Hoogland C, Ivanyi I, Appel RD, Bairoch A. ExPASy: The proteomics server for in-depth protein knowledge and analysis. *Nucleic. Acids Res.* 2003; **31:** 3784-8.
43. Brueggemann LI, Martin BL, Barakat J, Byron KL, Cribbs LL. Low voltage-activated calcium channels in vascular smooth muscle: T-type channels and AVP-stimulated calcium spiking. *Am. J. Physiol. Heart Circ. Physiol.* 2005; **288:** H923-35.
44. Bilmen JG, Michelangeli F. Inhibition of the type 1 inositol 1,4,5-trisphosphate receptor by 2-aminoethoxydiphenylborate. *Cell Signal* 2002; **14:** 955-60.
45. Knot HJ, Nelson MT. Regulation of arterial diameter and wall Ca^{2+} in cerebral arteries of rat by membrane potential and intravascular pressure. *J. Physiol.* 1998; **508:** 199-209.
46. Harder DR. Pressure-induced myogenic activation of cat cerebral arteries is dependent on intact endothelium. *Circ. Res.* 1987; **60:** 102-7.
47. Hansen PB, Jensen BL, Andreasen D, Friis UG, Skott O. Vascular smooth muscle cells express the α_{1A} subunit of a P-/Q-type voltage-dependent Ca^{2+} channel, and It is functionally important in renal afferent arterioles. *Circ. Res.* 2000; **87:** 896-902.
48. Andreasen D, Friis UG, Uhrenholt TR, Jensen BL, Skott O, Hansen PB. Coexpression of voltage-dependent calcium channels Cav1.2, 2.1a, and 2.1b in vascular myocytes. *Hypertension* 2006; **47:** 735-41.
49. Itonaga Y, Nakajima T, Morita H, *et al.* Contribution of nifedipine-insensitive voltage-dependent Ca^{2+} channel to diameter regulation in rabbit mesenteric artery. *Life Sci.* 2002;72:487-500.
50. Morita H, Sharada T, Takewaki T, Ito Y, Inoue R. Multiple regulation by external ATP of nifedipine-insensitive, high voltage-activated Ca^{2+} current in guinea-pig mesenteric terminal arteriole. *J. Physiol.* 2002; **539:** 805-16.
51. Evans J, Gelband CH. A novel Ca^{2+} channel in vascular smooth muscle? *Circ. Res.* 1999; **85:** 651-2.
52. Gustafsson F, Andreasen D, Salomonsson M, Jensen BL, Holstein-Rathlou N. Conducted vasoconstriction in rat mesenteric arterioles: role for dihydropyridine-insensitive Ca^{2+} channels. *Am. J. Physiol. Heart Circ. Physiol.* 2001; **280:** H582-90.
53. Jensen LJ, Salomonsson M, Jensen BL, Holstein-Rathlou NH. Depolarization-induced calcium influx in rat mesenteric small arterioles is mediated exclusively via mibefradil-sensitive calcium channels. *Br. J. Pharmacol.* 2004; **142:** 709-18.
54. Moosmang S, Schulla V, Welling A, *et al.* Dominant role of smooth muscle L-type calcium channel Cav1.2 for blood pressure regulation. *Embo. J.* 2003; **22:** 6027-34.
55. Feng MG, Li M, Navar LG. T-type calcium channels in the regulation of afferent and efferent arterioles in rats. *Am. J. Physiol. Renal Physiol.* 2004; **286:** F331-7.
56. Hayashi K, Wakino S, Homma K, Sugano N, Saruta T. Pathophysiological significance of T-type Ca^{2+} channels: role of T-type Ca^{2+} channels in renal

microcirculation. *J. Pharmacol. Sci.* 2005; **99:** 221-7.
57. Li J, Stevens L, Klugbauer N, Wray D. Roles of molecular regions in determining differences between voltage dependence of activation of $Ca_V3.1$ and $Ca_V1.2$ calcium channels. *J. Biol. Chem.* 2004; **279:** 26858-67.
58. Zhuang H, Bhattacharjee A, Hu F, *et al.* Cloning of a T-type Ca^{2+} channel isoform in insulin-secreting cells. *Diabetes* 2000; **49:** 59-64.
59. Perez-Reyes E. Molecular characterization of T-type calcium channels. *Cell Calcium* 2006; **40:** 89-96.

Received 1 April 2008, in revised form 30 April 2008. Accepted 5 May 2008.

Author for correspondence:

Professor Caryl E. Hill,
Division of Neuroscience,
John Curtin School of Medical Research,
Australian National University,
Canberra, ACT 2601, Australia.

Tel: +61 2 6125 2996
Fax: +61 2 6125 8077

E-mail: Caryl.hill@anu.edu.au